Takasu et al. J Musculoskelet Disord Treat 2016, 2:019
Volume 2 | Issue 3

Journal of
Musculoskeletal Disorders and Treatment

Original Research: Open Access

A Longitudinal Study of the Prediction of Pathologic Spinal Fractures in Multiple Myeloma with Trabecular Microarchitecture and CT-Based Finite Element Analyses

Miyuki Takasu[1]*, Chihiro Tani[1], Yoko Kaichi[1], Baba Yasutaka[1], Chikako Fujioka[1], Masao Kiguchi[1], Kumi Oshima[2], Yoshiaki Kuroda[2], Akira Sakai[3], Tatsuo Ichinohe[2] and Kazuo Awai[1]

[1]*Department of Diagnostic Radiology, Graduate School of Biomedical Sciences, Hiroshima University, Japan*

[2]*Department of Hematology and Oncology, Research Institute for Radiation Biology and Medicine, Hiroshima University, Japan*

[3]*Department of Radiation Life Sciences, Fukushima Medical University School of Medicine, Japan*

***Corresponding author:** *Miyuki Takasu, Department of Diagnostic Radiology, Graduate School of Biomedical Sciences, Hiroshima University, 1-2-3 Kasumi Minamiku Hiroshima, Japan, 734-8551, Tel: 81-82-257-5257, E-mail: my-takasu@syd.odn.ne.jp*

Abstract

Purpose: Sixty percent of myeloma patients develop pathologic fractures, with the majority occurring in the spine or ribs. The purpose of this study was to determine whether trabecular microstructural analysis can be used to predict new pathologic spinal fractures in myeloma patients.

Materials and methods: A total of 22 vertebral bodies from 14 patients with multiple myeloma were examined by 64-detector row CT prior to follow-up CT that showed new pathologic spinal fractures. Tissue bone mineral density (tBMD), trabecular parameters, and mechanical properties were calculated for three vertebrae, comprising a vertebra that would become fractured and the two adjacent vertebrae. Areas of lytic lesions were also obtained in the axial images containing the largest lytic lesions. For data analysis, univariate analysis was used to compare indices between vertebrae that would develop fractures and those that would not. Multivariate logistic regression analyses and receiver operating characteristic curves were also used.

Results: Univariate analysis demonstrated that area of lytic lesion, trabecular spacing, structure model index, tBMD, and failure load were significantly associated with the occurrence of pathologic fractures. Multivariate analysis identified area of lytic lesion, tBMD, and failure load as significant predictors of pathologic fractures. The area under the curve was 0.779 for failure load, 0.641 for tBMD, and 0.632 for area of lytic lesion.

Conclusion: Trabecular microstructural analysis can be used to predict new pathologic fractures in myeloma patients. Failure load and tBMD predict pathologic fractures better than the presence of a lytic lesion in a vertebra.

Keywords

CT-based finite element analysis, Pathologic spinal fracture, Multiple myeloma

Abbreviations

BMD: bone mineral density; MDCT: multidetector CT; FL: failure load; tBMD: tissue BMD; app BV/TV: apparent trabecular bone volume fraction; app Tb.Th: apparent trabecular thickness; app Tb.N: apparent trabecular number; app Tb.S: apparent trabecular separation; SMI: structure model index; FEM: finite element modeling; ROC: receiver operating characteristic

Introduction

Sixty percent of myeloma patients develop pathologic fractures, with the majority affecting the spine or ribs [1,2]. Patients with myeloma-associated vertebral fractures suffer from poorer quality of life than patients without fractures [3,4] and have been shown to have a significant reduction in overall survival [5].

In myeloma patients, reduced lumbar spine bone mineral density (BMD) correlates with increased risk for early vertebral fractures [6]. This makes dual-energy X-ray absorptiometry a valuable test because it may also influence the decision to begin bisphosphonate treatment, which can produce a 5-10% improvement over a 6-month period [7]. Although bone strength and fracture susceptibility are governed in large part by areal BMD, many other structural and material properties of bone, including microarchitecture, contribute considerably and independently to fragility [8-10].

Recently, high-resolution peripheral quantitative CT [11,12] and multidetector CT (MDCT) [13,14] have been used noninvasively to visualize the details of trabecular microarchitecture. In 2014, spinal microarchitecture and mechanical properties were examined in 74 patients with multiple myeloma using 64-detector row CT [15]. They obtained von Mises equivalent stress as failure load (FL), stiffness, microstructural parameters, and BMD, and they showed that patients with lower FL, stiffness, and BMD had a higher prevalence of vertebral fractures than other patients.

ClinMed International Library

Citation: Takasu M, Tani C, Kaichi Y, Yasutaka B, Fujioka C, et al. (2016) A Longitudinal Study of the Prediction of Pathologic Spinal Fractures in Multiple Myeloma with Trabecular Microarchitecture and CT-Based Finite Element Analyses. J Musculoskelet Disord Treat 2:019

Received: June 18, 2016: **Accepted:** August 13, 2016: **Published:** August 16, 2016

Table 1: Patients' characteristics.

Background data	Patients (n = 14)
Age (years)	62.1 ± 7.2
International staging system	
I	4
II	4
III	6
Monoclonal protein	
IgG	10
IgA	4
Concurrent chemotherapy	
Absent	0
Present	14
Months since diagnosis	9 [0-396]
Time between examinations (months)	9.4 ± 8.6
Use of ZA between examinations	
Absent	7
Present	7
Response to chemotherapy	
CR	0
PR (VGPR)	10 (1)
SD	3
PD	1

Data are presented as means ± SD or median [range], as appropriate. ZA: Zoledronic Acid; CR: Complete Remission; PR: Partial Response; VGPR: Very Good PR; SD: Stable Disease; PD: Progressive Disease.

Although CT scanning has proven to be superior in estimating fracture risk and instability to conventional X-rays [16], no longitudinal study has examined the occurrence of new vertebral fractures using clinical MDCT. The aim of the present study was to determine if certain cutoff values obtained from clinical MDCT-based microstructural and finite element analyses could be used in myeloma patients to predict pathologic fractures.

Materials and Methods

Participants

This retrospective, single-institution study was approved by an Institutional Review Board, with a waiver of informed consent.

The records of patients who had received whole-body MDCT for assessment of multiple myeloma were analyzed from 2009. The criteria used for the diagnosis of multiple myeloma were taken from the classification of the International Myeloma Working Group [17]. Then, all relevant images and reports were reviewed retrospectively to identify patients with at least one spinal fracture. All imaging studies relevant to the spine were retrospectively reviewed by one physician (M.T., 22 years of expertise in spinal imaging). Demographic information evaluated included patient age, concurrent chemotherapy, and years since diagnosis, time between two CT examinations, use of zoledronic acid, and response to chemotherapy (Table 1).

A total of 76 patients had concurrent MDCT imaging and a report of fracture. Of these patients, 4 men and 10 women met the inclusion criteria of at least one new vertebral fracture between two sequential MDCT examinations. Age ranged from 52 to 73 years, with an average of 62 years. These patients had a total of 114 MDCT examinations.

All patients had concurrent chemotherapy during two CT examinations. These regimens included melphalan-prednisone-bortezomib, doxorubicin-vincristine-dexamethasone, bortezomib-cyclophosphamide-dexamethasone, cyclophosphamide, and vorinostat. Patient treatment followed the standard practice at our institution. After initial treatment, patients received maintenance therapy with bortezomib or lenalidomide with or without zoledronic acid, as deemed appropriate by the treating physicians. Seven patients in the present study had concomitant zoledronic acid during the same periods. Ten of 14 patients had a partial response to chemotherapy.

Nine patients had one new fracture, three patients had two new fractures, one patient had three new fractures, and one patient had four new fractures.

Fracture definitions

All spinal levels on each exam from C2 to L5 were evaluated for the presence or absence of fractures and focal lesions. The Genant criteria [18] were used to identify and classify fracture types and grades as: "A", anterior wedge; "B", mid end-plate deformity, or "C", posterior wedge/crush. Genant grades were assigned as: grade 1, < 25% deformity; grade 2, deformity between 25% and 40%; and grade 3, deformity > 40%.

Imaging by MDCT

Bone lesions and extraskeletal disease were evaluated by whole-body non-contrast-enhanced CT according to the 2009 International Myeloma Working Group consensus statement [19]. The methods used to obtain trabecular microstructural indices have been described elsewhere [13]. Briefly, the whole body was scanned using the same CT unit and protocol as the specimen study described above. The three vertebrae that included the one vertebra that would become fractured and the two adjacent vertebrae were analyzed.

To obtain tissue BMD (tBMD) data by MDCT, the patients were scanned simultaneously with a bone mineral reference phantom (B-MAS2000; KYOTOKAGAKU Co., Kyoto, Japan) containing calibration objects with equivalent densities of 0, 50, 100, 150, and 200 mg/cm^3 calcium hydroxyapatite.

MDCT-based microstructural analyses

For microstructural analyses, the volume of interest (VOI) was defined manually as a 10 mm thickness of the central part of the vertebral body to avoid the cortex, the basivertebral foramen, and both endplates. The VOI was chosen in axial, reformatted sagittal and coronal planes to ensure that the sections were parallel to the endplates. Microstructural parameters were calculated using the same computer program as the specimen study, as described elsewhere [11]. A calibration curve to convert Hounsfield units of CT images to BMD units (g/cm^3) was generated using the bone mineral reference phantom. The calibration curve could subsequently be used to obtain BMD units for bone imaged with the CT systems. Using a volumetric BMD value for trabecular bone, > 178 mg/cm^3 within the bone marrow was extracted. Then, this threshold level was adopted for all extractions of cancellous bones. The following trabecular microstructural parameters were obtained: apparent trabecular bone volume fraction (app BV/TV), apparent trabecular thickness (app Tb.Th), apparent trabecular number (app Tb.N), apparent trabecular separation (app Tb.S), Euler's number, degree of anisotropy, and the structure model index (SMI). Details of these methods are described elsewhere [14].

MDCT-based finite element analysis

Finite element modeling (FEM) was performed using a computer program for a 3D image analysis system (TRI/3D-BON; RATOC System Engineering, Tokyo, Japan), which separates the VOI into the cortical and trabecular bone portions. Three-dimensional (3D) finite element models were constructed from the CT data. A global threshold algorithm was used to extract the bone area with a threshold of 178 mg/cm^3. Materially nonlinear finite element analyses were performed. In FL analysis, von Mises stress > 68 MPa was defined as the stress that induces trabecular fracture. FL was determined to the level that induces fractures in 2.8% of trabecular bone. A finite element model was created using a 0.2 mm isometric hexagonal mesh from pixels that constituted the trabecular bone [20]. Octahedral elements were adapted to represent the smooth surface. For trabecular bone, Young's modulus was determined using Carter's equation and the volumetric BMD value [21]. Poisson's ratio was set as 0.3 for all trabecular bone. The distal part of vertebral trabecular bone was fixed, and compressed simulation was applied at a load of 500 N from the proximal section.

Table 2: Data for all 14 patients with 24 new pathologic fractures.

Patient No.	Age (y)	Sex	Lytic lesion (mm^2)	Vertebral level	Fracture type
1	65	F	0	L1	A1
2	67	M	0	L3	A2
3	68	M	59	L2	A3
4	63	M	0	L1	A3
5	66	F	50	Th7	A3
			0	Th11	A3
			0	Th12	A3
			17	L2	A3
6	53	F	99	Th5	B2
			119	Th7	B2
7	57	F	0	Th10	A2
8	50	F	98	Th4	A2
			0	Th5	B2
			300	L5	B2
9	60	F	16	Th8	A2
			40	Th9	B1
10	67	F	0	Th9	B1
11	73	F	0	L4	B2
12	52	F	22	Th6	A2
13	59	M	0	Th8	B2
			0	Th11	B2
14	70	F	9	L1	A2

Table 3: Values of tBMD, trabecular microstructural parameters, and mechanical properties.

	Vertebrae that would fracture	Vertebrae that would not fracture
Number of vertebrae	22	41
Lytic lesion (mm^2)	41.7 ± 70.3**	9.8 ± 26.8
tBMD	78.5 ± 26.5	84.1 ± 31.4
Ratio to mean value	-3.5 ± 7.9*	1.9 ± 11.0
Microstructural parameters		
App BV/TV (%)	29.1 ± 10.0	30.9 ± 11.7
Ratio to mean value	-3.1 ± 8.3*	1.7 ± 10.7
App Tb.N ($1/mm^3$)	0.31 ± 0.07	0.32 ± 0.07
Ratio to mean value	-2.0 ± 6.9	1.1 ± 9.2
App Tb.Th (μm)	703.0 ± 116.2	707.5 ± 109.2
Ratio to mean value	-0.35 ± 3.8	0.18 ± 5.3
App Tb.S (μm)	877.3 ± 228.3	859.6 ± 250.7
Ratio to mean value	1.9 ± 6.2*	-1.0 ± 6.9
SMI	1.73 ± 0.36	1.66 ± 0.44
Ratio to mean value	3.9 ± 10.0**	-2.1 ± 7.5
Euler's number	-877.5 ± 626.0	-981.4 ± 694.6
Ratio to mean value	0.72 ± 25.5	-0.39 ± 41.2
Degree of anisotropy	1.45 ± 0.19	1.43 ± 0.23
Ratio to mean value	1.0 ± 2.8	-0.53 ± 5.3
Mechanical properties		
Failure load (N)	2754 ± 1758	2898 ± 1576
Ratio to mean value	-7.8 ± 16.9**	4.2 ± 18.0

Data are means ± SD. Ratio to mean values are mean percent change ± SD. tBMD: Tissue Bone Mineral Density; Ratio to mean value, Ratio to mean value from the three adjacent vertebrae; app BV/TV: Apparent Bone Volume Per Tissue Volume; App Tb.N: Apparent Trabecular Number; App Tb.Th: Apparent Trabecular Thickness; App Tb.S: Apparent Trabecular Spacing; SMI: Structure Model Index.

**$p < 0.05$, *$p < 0.01$

Areas of lytic lesion measurements

Areas of lytic lesions were obtained by manually drawn regions of interest in the axial images that contained the largest lytic lesions for each of the three vertebrae.

Statistical Analysis

Tissue bone mineral density (tBMD), trabecular parameters, and mechanical properties were calculated for three vertebrae, comprising a vertebra that would become fractured and the two adjacent vertebrae. Trabecular microstructural indices were expressed as ratios to mean values from the three vertebrae.

For data analysis, univariate analysis was used to compare indices between vertebrae that would develop fractures and those that would not. Multivariate logistic regression analyses and receiver operating characteristic (ROC) curves were also used. Variables showing values of $P < 0.05$ on univariate analysis were included in the multivariate analysis. The cutoff value to predict pathologic fractures was determined by ROC analysis.

All analyses were performed with a spreadsheet application (Microsoft Office Excel 2010, Redmond, WA). Values of $P < 0.05$ were considered significant.

Results

Fractures

There were 22 new vertebral body fractures identified, with an average of 1.6 per patient (range 1-4). The distribution of the fractures is shown in table 2. Most fractures involved the lower thoracic and lumbar levels. The "Genant" B2-type of fractures was the most common (7 fractures), followed by A2- and A3-type fractures (6 fractures).

Table 4: Multivariate regression analysis examining the effects of trabecular microstructural indices and mechanical properties on fracture occurrence.

Variable	*β ± Standard error	*P* Value	Odds ratio (CI)
Lytic lesion	0.021 ± 0.01	0.04	1.02 (1.00, 1.04)
tBMD	-0.34 ± 0.17	0.04	0.71 (0.51, 0.99)
Failure load	-0.042 ± 0.02	0.02	0.96 (0.93, 0.99)

*β: Standardized partial regression coefficient; tBMD: Tissue Bone Mineral Density.

Table 5: Receiver operating characteristic curves to evaluate the diagnostic performance of contributors to fractures.

Variable	AUC	Sensitivity (%)	Specificity (%)	Cut-off values
Lytic lesion	0.632	50 (12/22)	77.5 (31/40)	16 mm^2
tBMD	0.641	68.2 (15/22)	80.0 (32/40)	-5.6%
Failure load	0.779	72.7 (16/22)	82.5 (33/40)	-9.4%

AUC: Area Under The Curve; tBMD: Tissue Bone Mineral Density.

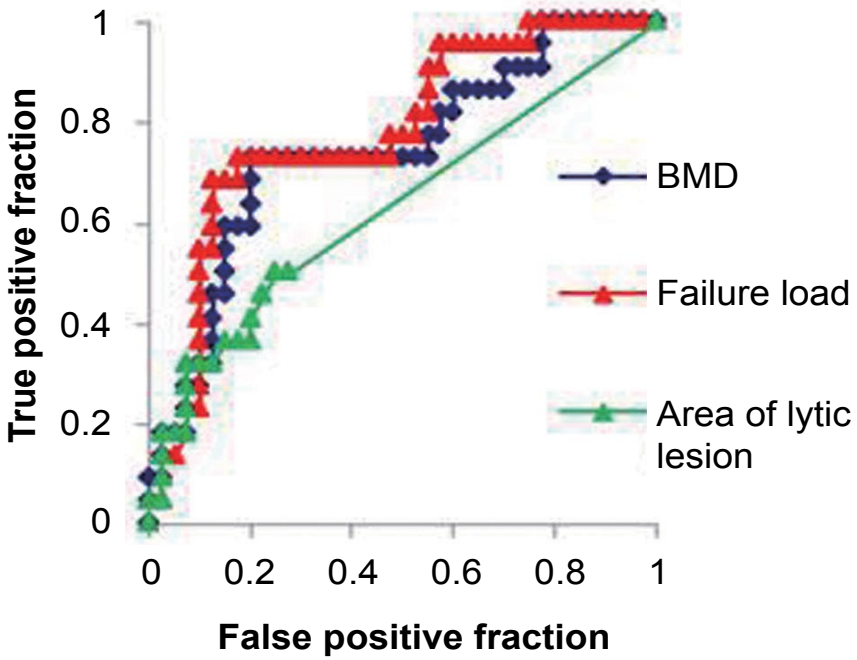

Figure 1: ROC curves for identifying the AUC having discriminatory power to distinguish vertebrae that would become fractured from those that would not. Failure load, with an optimal cutoff value of -9.4%, had the highest discriminatory power between them. BMD: tissue bone mineral density.

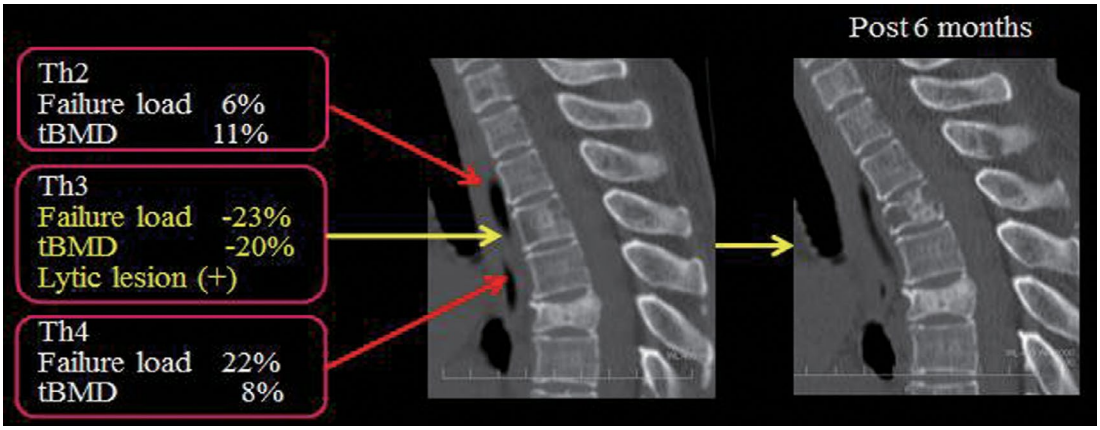

Figure 2: Sagittal reconstructed multidetector CT images of the spine (A) before and (B) 6 months after bortezomib therapy obtained in a 50-year-old woman with partial response to chemotherapy. The third thoracic vertebra has a failure load of -23% and a tBMD of -20% compared to the adjacent two vertebrae. A lytic lesion is also seen. After 6 months, this vertebra fractured. Th: thoracic.

MDCT-based microstructural analysis and finite element modeling

In table 3, tBMD, microstructural parameters, and FL of the 2 groups (vertebrae that would fracture and vertebrae that would not fracture) are summarized. Area of lytic lesions, app Tb.S, and SMI were significantly higher in the vertebrae that would fracture than in the vertebrae that would not fracture. Tissue BMD, App BV/TV, and FL were significantly lower in the vertebrae that would fracture than in the vertebrae that would not fracture. There were no significant differences in app Tb.N, app Tb.Th, Euler's number, and degree of anisotropy between the 2 groups.

The following factors were introduced in multivariate analysis: lytic lesion, tBMD, app BV/TV, app Tb.S, SMI, and FL. Multivariate analysis identified area of the lytic lesion, tBMD, and FL as significant predictors of pathologic fractures (Table 4).

The AUC having the highest discriminatory power to distinguish vertebra that would become fractured from those would not was FL (AUC = 0.779; 95% confidence intervals (CIs, 0.647, 0.876), with an optimal cutoff value of -9.4%; the sensitivity and specificity were 72.7% (CIs, 0.603, 0.852) and 82.5% (CIs, 0.619, 0.982), respectively (Table 5 and Figure 1). The AUC for tBMD was 0.641 (CIs, 0.598, 0.846), with an optimal cutoff value of -0.56%; the sensitivity and specificity were 68.2% (CIs, 0.549, 0.815) and 80.0% (CIs, 0.598,

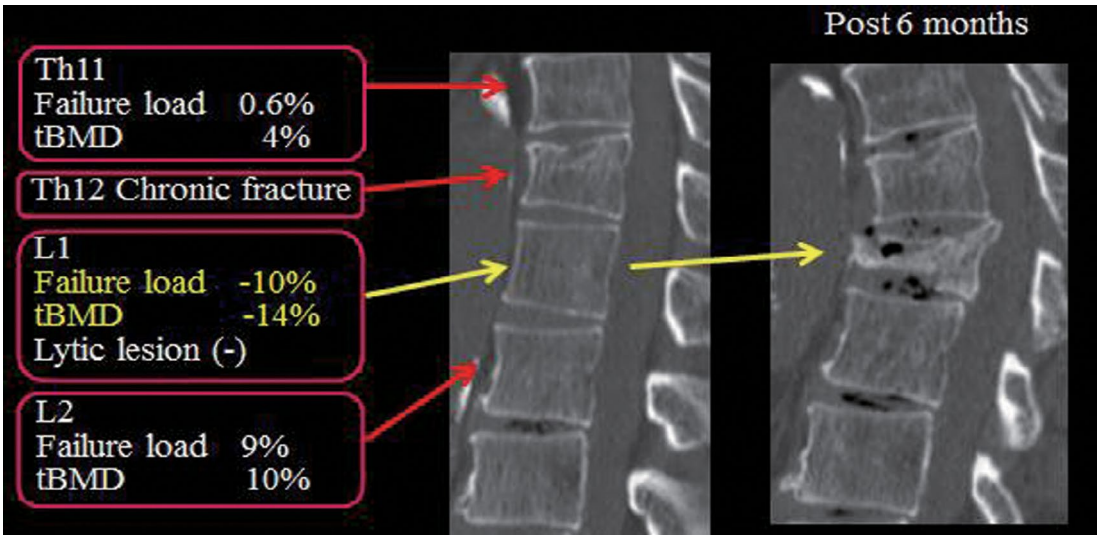

Figure 3: Sagittal reconstructed multidetector CT images of the spine (A) before and (B) 6 months after bortezomib therapy obtained in a 63-year-old man with partial response to chemotherapy. The first lumbar vertebra has a failure load of -10% and a tBMD of -14% compared to the adjacent two vertebrae, but had no lytic lesion. After 6 months, this vertebra fractured. L: lumbar.

0.989), respectively. The AUC for lytic lesion was 0.632 (CIs, 0.434, 0.830), with an optimal cutoff value of 16 mm^2; the sensitivity and specificity were 50.0% (CIs, 0.349, 0.651) and 77.5% (CIs, 0.592, 0.958), respectively. Representative images are shown in figure 2 and figure 3.

Discussion

Osteoporosis is a chief manifestation of myeloma and up to 90% of patients with myeloma develop vertebral complications such as fractures [22]. Although several independent prognostic markers have been identified to predict overall survival and progression from asymptomatic myeloma to symptomatic myeloma, vertebral fractures are still difficult to predict.

Several reports describe the use of radiological procedures to predict pathologic fractures at a variety of skeletal sites in myeloma patients [23,24]. MRI can also be used to predict the risk for vertebral fracture. Patients with advanced myeloma with more than 10 lesions on spinal MRI had a 6- to 10-fold higher risk of fracture than patients who had a normal appearance or fewer than 10 lesions on MRI [25]. Recently, Merz et al. performed dynamic contrast-enhanced MRI of the lumbar spine in 131 myeloma patients to acquire amplitude A and exchange rate constant *k*ep [22]. They demonstrated that higher baseline *k*ep values were associated with decreased vertebral height on a second MRI, and A values were associated with new vertebral fractures in the lower lumbar spine. Their scheme to predict the risk of fracture by spinal level, which had not been reported in the literature, is useful and practical in the follow-up of myeloma patients. However, care should be taken when using contrast agents in myeloma patients because patients with reduced renal function are at risk of developing nephrogenic systemic fibrosis after contrast-enhanced MRI.

In 2011, Mulligan et al. reported that the combination of diffuse or multifocal MR patterns and standardized uptake value > 3.5 was seen at 7 vertebral levels, all but one with new pathologic fractures [26]. However, performing these two modalities is expensive and sometimes is not covered by insurance. Although a previous study has shown that clinical MDCT was useful for the prediction of subsequent fractures after vertebroplasty [27], prediction of vertebral fractures by clinical MDCT in multiple myeloma has not been described previously, and it might have clinical implications for treatment planning in cases of impending fractures.

As the present results have shown, a FL cut off of -9.4% below the mean value was helpful for identifying at-risk vertebral levels in myeloma patients. In the present series, 16 of 22 vertebral levels that had a FL deviation < -9.4% from the mean value had a new fracture within a mean time of 9.4 months. The remaining six vertebrae had fractures with a FL deviation > -9.4% from the mean value. The information on lytic lesions in the vertebrae may also be helpful to predict the likelihood of impending fracture development. Five of six vertebrae that would fracture and had FL deviation > -9.4% from the mean value had visible lytic lesions. None of 16 vertebral levels with a FL deviation > 5% and no lytic lesions fractured. These results show that vertebral bodies that do not have a lytic lesion might fracture, and MDCT-based FEM could predict vertebral fractures by spinal level.

The present study has several limitations, including a relatively small number of new fractures and a lack of pathologic proof of the nature of each vertebral fracture. Although diagnosis in all of our patients was confirmed by obtaining bone marrow samples of the iliac crest, there may be some heterogeneity of tumour infiltration among bones. We acknowledge that it may have some effect on our findings. In addition, the speed of bone loss might have been different in each patient because of the diversity of concomitant chemotherapy. Seven patients in the present study had concomitant zoledronic acid during two CT examinations. The use of zoledronic acid could improve bone strength but the small number of patients with new vertebral body fractures did not allow us to evaluate the difference of trabecular indices between the patients with or without zoledronic acid. No recommendation regarding follow-up interval cannot be made. A larger, longitudinal study would allow a more precise prediction of new pathologic fractures in myeloma patients.

Conclusion

The present results indicate that vertebrae with FL of < -9.4% compared to two adjacent vertebrae and lytic lesions of > 16 mm^2 are at risk of imminent fracture. Early intervention may prevent or delay the development of a fracture. If larger prospective studies confirm this association, preventive measures such as bisphosphonates should be considered regardless of presence of osteolytic bone lesions on CT. Radiotherapy or vertebroplasty could also be considered to try to avoid the development of a pathologic fracture.

Acknowledgments

M.T. is supported by Japan and International Myeloma Foundation Japan's Research Grants 2012, which provided funding for the Japan Myeloma Study Group, 35 Gengo Moriokamachi Obushi Aichi, Japan. They had no role in the conduct of this research.

Disclosure

The authors have stated that they have no conflicts of interest.

References

1. Palumbo A, Anderson K (2011) Multiple myeloma. N Engl J Med 364: 1046-1060.

2. Melton L, Kyle R, Achenbach S, Oberg AL, Rajkumar SV (2005) Fracture risk with multiple myeloma: a population based study. J Bone Miner Metab 20: 487-493.

3. Julka A, Tolhurst SR, Srinivasan RC, Graziano GP (2014) Functional outcomes and height restoration for patients with multiple myeloma-related osteolytic vertebral compression fractures treated with kyphoplasty. J Spinal Disord Tech 27: 342-346.

4. Berenson J, Pflugmacher R, Jarzem P, Zonder J, Schechtman K, et al. (2011) Balloon kyphoplasty versus non-surgical fracture management for treatment of painful vertebral body compression fractures in patients with cancer: a multicentre, randomised controlled trial. Lancet Oncol 12: 225-235.

5. Sonmez M, Akagun T, Topbas M, Umit Cobanoglu, Bircan Sonmez, et al. (2008) Effect of pathologic fractures on survival in multiple myeloma patients: a case control study. J Clin Cancer Res 27: 11-14.

6. Abildgaard N, Brixen K, Eriksen EF, Kristensen JE, Nielsen JL, et al. (2004) Sequential analysis of biochemical markers of bone resorption and bone densitometry in multiple myeloma. Haematologica 89: 567-577.

7. Mulligan ME, Badros AZ (2007) PET/CT and MR imaging in myeloma. Skeletal Radiol 36: 5-16.

8. Laib A, Hauselmann HJ, Ruegsegger P (1998) *In vivo* high resolution 3D-QCT of the human forearm. Technol Health Care 6: 329-337.

9. Laib A, Ruegsegger P (1999) Comparison of structure extraction methods for *in vivo* trabecular bone measurements. Comput Med Imaging Graph 23: 69-74.

10. Cheung AM, Detsky AS (2008) Osteoporosis and fractures: missing the bridge? JAMA 299: 1468-1470.

11. Stein EM, Liu XS, Nickolas TL, Cohen A, McMahon DJ, et al. (2012) Microarchitectural abnormalities are more severe in postmenopausal women with vertebral compared to nonvertebral fractures. J Clin Endocrinol Metab 97: E1918-E1926.

12. Boutroy S, Bouxsein ML, Munoz F, Delmas PD (2005) *In vivo* assessment of trabecular bone microarchitecture by high-resolution peripheral quantitative computed tomography. J Clin Endocrinol Metab 90: 6508-6515.

13. Takasu M, Tani C, Ishikawa M, Date S, Horiguchi J, et al. (2011) Multiple myeloma: microstructural analysis of lumbar trabecular bones in patients without visible bone lesions--preliminary results. Radiology 260: 472-479.

14. Ito M, Ikeda K, Nishiguchi M, Shindo H, Uetani M, et al. (2005) Multi-Detector Row CT Imaging of Vertebral Microstructure for Evaluation of Fracture Risk. J Bone Miner Res 20: 1828-1836.

15. Takasu M, Kaichi Y, Awai K, Asaoku H, Kuroda Y, et al. (2014) Vertebral fracture risk of multiple myeloma assessed by a CT-based finite element and trabecular structure analysis. Clin Lymphoma Myeloma Leuk 14: 12-13.

16. Horger M, Claussen CD, Bross-Bach U, Vonthein R, Trabold T, et al. (2005) Whole-body low-dose multidetector row-CT in the diagnosis of multiple myeloma: an alternative to conventional radiography. Eur J Radiol 54: 289-297.

17. International Myeloma Working Group (2003) Criteria for the classification of monoclonal gammopathies, multiple myeloma and related disorders: a report of the International Myeloma Working Group. Br J Haematol 121: 749-757.

18. Genant HK, Wu CY, van Kuijk C, Nevitt MC (1993) Vertebral fracture assessment using a semi-quantitative technique. J Bone Miner Res 8: 1137-1148.

19. Dimopoulos M, Terpos E, Comenzo RL, Tosi P, Beksac M, et al. (2009) IMWG: International Myeloma Working Group consensus statement and guidelines regarding the current role of imaging techniques in the diagnosis and monitoring of multiple myeloma. Leukemia 23: 1545-1556.

20. Ulrich D, Riebergen B, Laib A, Rüegsegger P (1998) Mechanical analysis of bone and its microarchitecture based on *in vivo* voxel images. Technol Health Care 6: 421-427.

21. Carter DR, Hayes WC (1977) The compressive behavior of bone as a two-phase porous structure. J Bone Joint Surg Am 59: 954-962.

22. Merz M, Moehler TM, Ritsch J, Bäuerle T, Zechmann CM, et al. (2015) Prognostic significance of increased bone marrow microcirculation in newly diagnosed multiple myeloma: results of a prospective DCE-MRI study. Eur Radiol Jul 26: 1404-1411.

23. Bredella M, Essary B, Torriani M, Ouellete H, Palmer W (2008) Use of FDG-PET in differentiating benign from malignant compression fractures. Skeletal Radiol 37: 405-413.

24. Shin D, Shon O, Byun S, Choi J, Chun K, et al. (2008) Differentiation between malignant and benign pathologic fractures with F-18-fluoro-2-deoxy-D-glucose positron emission tomography/ computed tomography. Skeletal Radiol 37: 415-421.

25. Lecouvet FE, Malghem J, Michaux L, Michaux JL, Lehmann F, et al. (1997) Vertebral compression fractures in multiple myeloma. Part II. Assessment of fracture risk with MR imaging of spinal bone marrow. Radiology 204: 201-205.

26. Mulligan M, Chirindel A, Karchevsky M (2011) Characterizing and predicting pathologic spine fractures in myeloma patients with FDG PET/CT and MR imaging. Cancer Invest 29: 370-376.

27. Hiwatashi A, Yoshiura T, Yamashita K, Kamano H, Dashjamts T, et al. (2009) Subsequent fracture after percutaneous vertebroplasty can be predicted on preoperative multidetector row CT. AJNR Am J Neuroradiol 30: 1830-1834.